EURODYN 2020
XI International Conference on Structural Dynamics
M. Papadrakakis, M. Fragiadakis, C. Papadimitriou (eds.)
Athens, Greece, 22–24 June 2020

MODAL IDENTIFICATION OF STRUCTURES DURING STATIC LOAD TESTING: INTERACTION EFFECTS.

Antolin Lorenzana[1*], Alvaro Magdaleno[1], Tomislav Jarak[1], Roberto Martinez[2], Antonio Balmori[2], Luis-AlfonsoBasterra[2], Lara del Val[3], Juan J. Villacorta[3], Alberto Izquierdo[3]

[1] ITAP. Universidad de Valladolid
Paseo del Cauce, 59, 47011 Valladolid, Spain
alvaro.magdaleno@uva.es, ali@eii.uva.es

[2]Research Group of Timber Structures and Wood Technology, University of Valladolid
Avenida de Salamanca, 18, 47014 Valladolid, Spain
(robertomartinez, balmori, basterra)@arq.uva.es

[3]Signal Theory and Communications Department, University of Valladolid
Campus Miguel Delibes, 47011 Valladolid, Spain
(larval, juavil, alberto.izquierdo)@tel.uva.es

Keywords: structural dynamics; experimental modal analysis, solid or liquid live loads.

Abstract. *Structures such as floors or bridges are usually tested, according to some standards, in order to check some of their properties. Stiffness and modal parameters can be obtained through static and dynamic testing. Usually, static testing consists in adding mass to the structure and measuring the additional deflection. For convenience reasons, the added mass is usually implemented with tanks of water. However, if the static testing scenario is used to conclude modal parameters or dynamic serviceability assessment, it is necessary to ensure that the added load is representative of the structure conditions during its life span. Although for static load testing the results do not depend on the nature of the gravitational load, the same does not occur when modal parameters are of interest. Whether the mass is solid (sandbags or concrete blocks), liquid (water in tanks) or other types (as vehicles or people, etc.) greatly affects the damping due to interaction phenomena. These interaction effects appeared in an attempt to evaluate the damping on a wooden floor through traditional techniques (modal analysis using a shaker and some accelerometers). With the floor without any load, the different modes of their girders (one-way slab floor) could be easily identified and their frequencies and damping ratios well quantified. However, when supporting water tanks, the identification procedure was a challenging task. Trying to understand how the nature (solid or liquid) of the added mass affects, six case studies based on a lab-scale structure are presented.*

1 INTRODUCTION

Figure 1 shows a load test on a pedestrian timber bridge. It consists of distributing several water-filled tanks along its length and measuring the increase in deflection to obtain the stiffness of the structure. Taking advantage of the instrumentation carried out, could a modal analysis be made to obtain the modal properties (frequency and damping ratios) of the footbridge in crowded conditions? In the same way, figure 2 shows a full-scale laboratory timber floor. For the same load, the modal properties are very different if the load is just water in a pool (left) or people. Even if people are sitting (center) or standing (right) the results are also very different.

Figure 1. Loading test in a timber footbridge.

Figure 2. Different loading conditions in a timber floor.

Trying to understand how the nature of the added mass affects, figure 3 shows two scale models (a “bridge” and a “2-storey building”) on which tests are being carried out by loading these models with water balloons and inducing vertical vibrations (for the bridge) or horizontal vibrations (for the 2-storey building). In both cases, tests can be carried out by means of the standard instrumentation consisting on an impact (over a load cell) and several accelerometers, all the signals been recorded by a proper data-logger. Processing all the data (experimental modal analysis methodology, EMA, [1, 2]), mode shapes, modal damping and natural frequencies can be obtained by identification techniques [3, 4, 5].

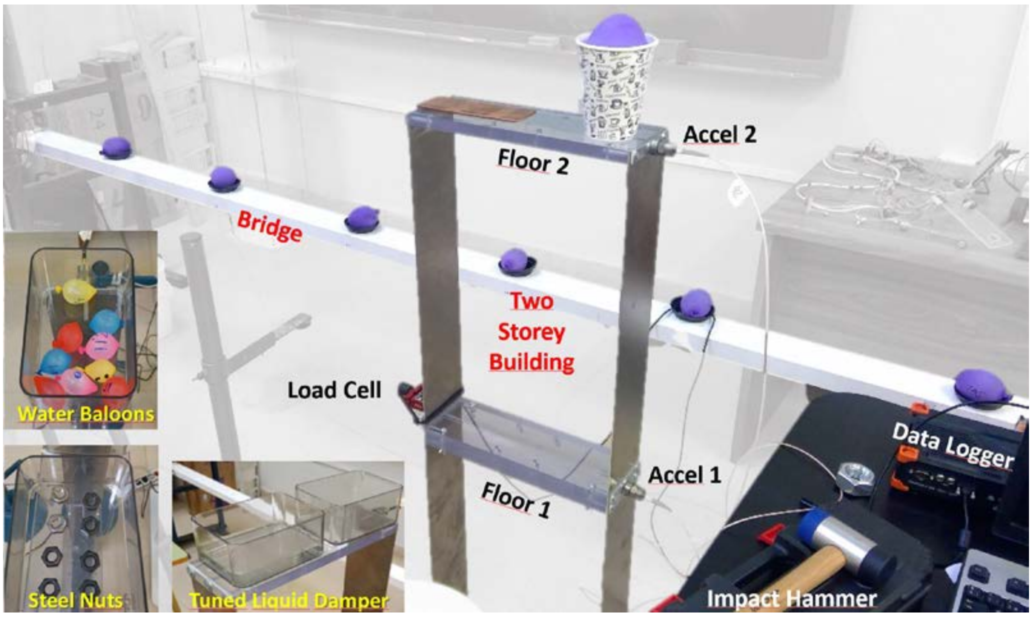

Figure 3. Lab layout.

2 CASE STUDIES DESCRIPTION

In order to design a controlled lab test and to identify the interaction effects, the model of a 2-storey building (figure 3) is used. Each floor consists of a methacrylate plate rigid enough to suppose them to be rigid bodies for the purposes of this work. They are connected to each other and to the ground *via* two aluminium plates. These plates, very stiff in one bending direction with respect to the other, limit the movement of the building model to one horizontal direction.

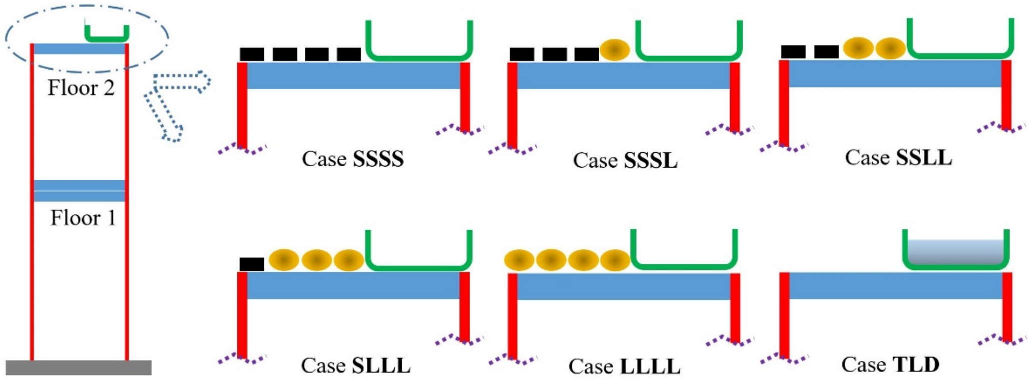

Figure 4. Scenarios under study.

Six case studies are presented (figure 4). As a reference or blank scenario, 16 steel nuts of 0.010 kg each were added on the second floor (accounting for 18% of the total mass of the floor, the first floor weighs twice as much). After that, 4 of the nuts were replaced by 4 balloons containing the same mass in water. Later, the same with another 4 nuts and so on until the solid masses were all replaced. In the last scenario, nuts and balloons are replaced by a tank containing the same mass in water, constituting a tuned liquid damper (TLD). In figure 3, at left, nuts, balloons and the TLD can be seen. Case SSSS corresponds to the case where all the added mass is solid (nuts). In the SSSL case one quarter of the solid mass is replaced by the equivalent in water (confined in balloons). In the SSLL case half of the added mass is solid and half is liquid. Finally, in the SLLL case the added mass is one-quarter solid and three-quarters liquid and in the case LLLL case all the added mass is liquid.

3 METHODOLOGY

As can be guessed in figure 5, left, two IEPE accelerometers (100 mV/g) are installed on each floor (blue ring), both oriented to measure horizontal accelerations. The excitation consists of an impact applied to the load cell (100 N max.), also installed in floor 1 (red ring). The accelerometers and the load cell are wired to an acquisition system (SIRIUS model of the brand Dewesoft), and data are registered at 400 samples per second. In figure 5 right, FRF (H_1 estimator) are obtained after each impact and several averages (3 or 4) are carried out in order to remove some of noise.

Figure 5. Modal analysis on air.

Both FRFs (the one corresponding to the first floor or auto-FRF and the one of the second floor) (are fitted in magnitude and in phase) to a theoretical system of 2 degrees of freedom (eq. 1), in which a general viscous damping model has been assumed.

$$H_{jk}(\omega) = \sum_{r=1}^{m} \left(\frac{\theta_{rj}\theta_{rk}}{i\omega - s_r} + \frac{\theta_{rj}^{*}\theta_{rk}^{*}}{i\omega - s_r^{*}} \right) \quad (1)$$

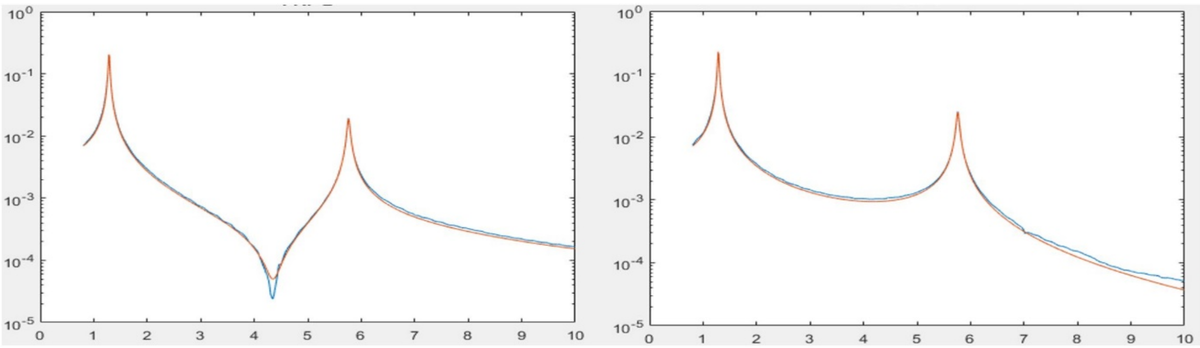

Figure 6. Case SSSS: FRF of the first floor (left) and of the second floor (right)

For the reference case (SSSS), figure 6 shows the experimental FRFs (in blue) and their corresponding fitted curves (in red) when m=2. As can be seen, the system fits perfectly with a two-dof, as intended. After the curve-fitting process, table 1 shows the modal parameters, including the modal coordinates of the two modes, that are plotted in figure 7.

	Frequency (Hz)	Damping (%)	Modal coordinates	
			floor1	**floor2**
Mode 1	1.289	0.0104	-0.0948 + 0.0926i	-0.1042 + 0.0984i
Mode 2	5.764	0.0053	-0.0419 + 0.0393i	0.0593 - 0.0493i

Table 1. Case SSSS after curve fitting and mode shape identification.

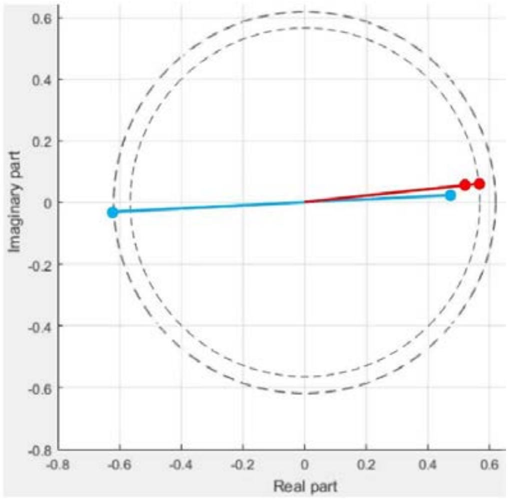

Figure 7. Argand plot for modes 1 (red) and 2 (blue)

	ω1	**Peak_floor1**	**Peak_floor2**	**ξ1**	**ω2**	**Peak_floor1**	**Peak_floor2**	**ξ2**
SSSS	1.289	13.622	14.736	0.0104	5.764	22.638	30.354	0.0053
SSSL	1.297	9.822	11.143	0.0140	5.817	14.329	20.385	0.0081
SSLL	1.301	7.329	8.606	0.0184	5.869	12.166	16.143	0.0100
SLLL	1.306	6.228	7.359	0.0220	5.915	9.746	12.843	0.0129
LLLL	1.298	6.162	6.649	0.0238	5.970	5.683	8.850	0.0195
TLD_a	1.171	1.498	1.906	0.0430	6.000	15.999	32.260	0.0053
TLD_b	1.422	1.536	1.736	0.1211				

Table 2. Modal parameter and accelerance values.

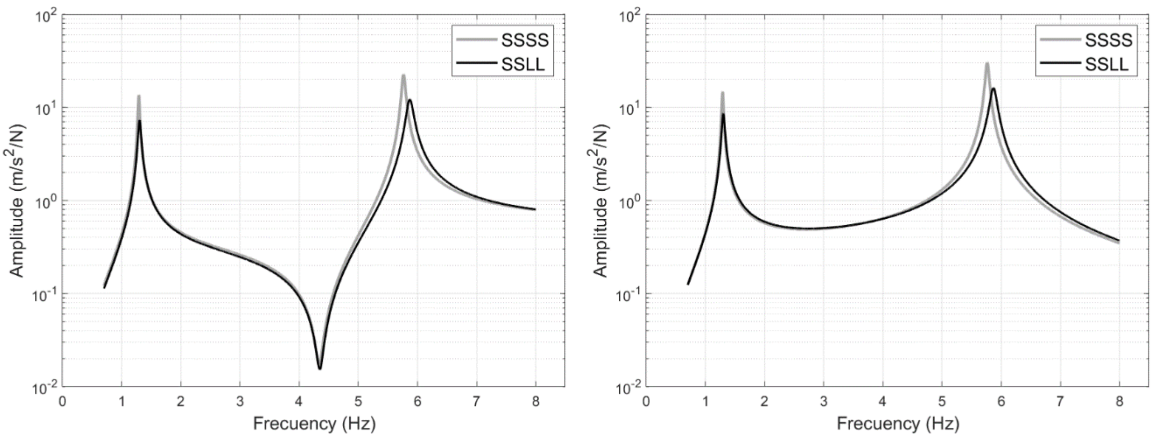

Figure 8. Case SSLL: FRF of the first floor (left) and of the second floor (right)

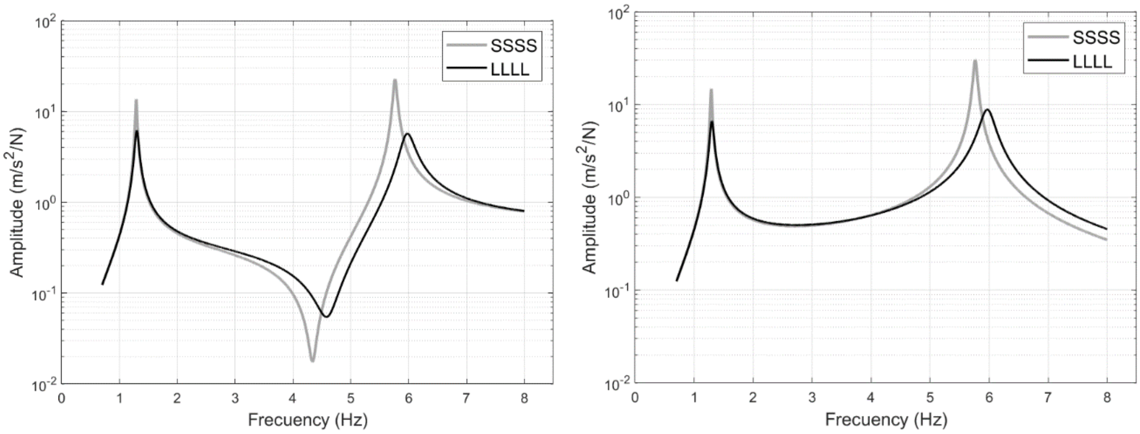

Figure 9. Case LLLL: FRF of the first floor (left) and of the second floor (right)

4 RESULTS

Following a similar procedure for the rest of the cases, results of table 2 and table 3 are obtained. Figure 8 shows the adjusted curves for the SSLL case and figure 9 for the LLLL case. In both cases, the adjusted curves for the SSSS case are shown in grey. Table 2 also shows the values of the accelerance of both FRFs (floor 1 and floor 2) for the peaks corresponding to mode 1 and mode 2. All these values are drawn in the graphs in figure 11.

	Mode shape 1		Mode shape 2	
	floor1	floor2	floor1	floor2
SSSS	-0.0948 + 0.0926i	-0.1042 + 0.0984i	-0.0419 + 0.0393i	0.0593 - 0.0493i
SSSL	-0.0933 + 0.0903i	-0.1069 + 0.1013i	-0.0405 + 0.0389i	0.0610 - 0.0520i
SSLL	-0.0911 + 0.0906i	-0.1110 + 0.1020i	-0.0409 + 0.0403i	0.0572 - 0.0506i
SLLL	-0.0908 + 0.0919i	-0.1136 + 0.1018i	-0.04313 + 0.0409i	0.0568 - 0.0517i
LLLL	-0.0963 + 0.0932i	-0.1069 + 0.0973i	-0.0390 + 0.0375i	0.0624 - 0.0587i
TLD	0.0776 - 0.0097i -0.0692 + 0.1141i	0.0960 - 0.0348i -0.0843 + 0.1115i	0.0341 - 0.0331i	-0.0689 + 0.0650i

Table 3. Modal coordinates.

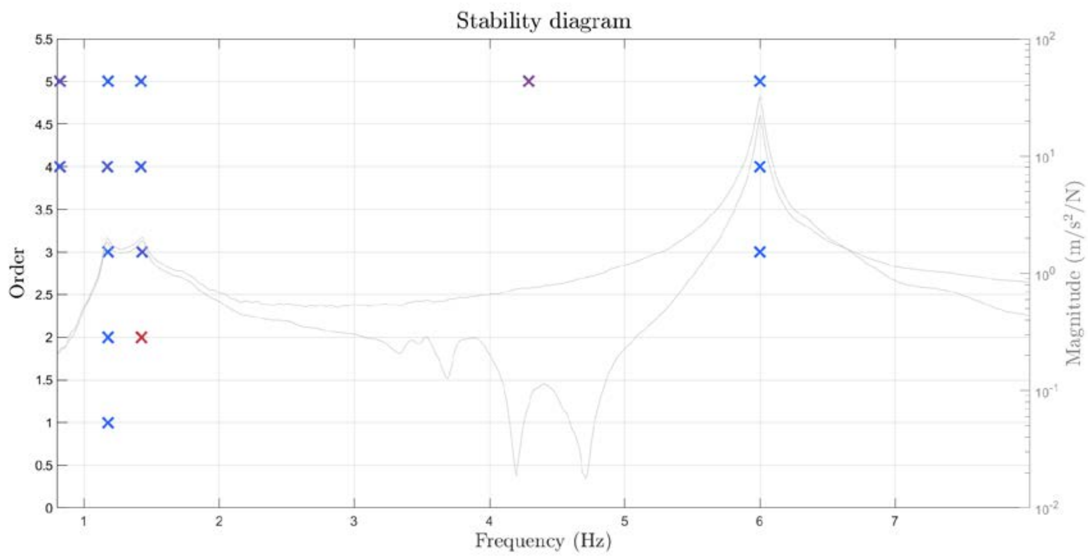

Figure 10a. Case TLD: Stability diagram.

Actually, the adjustment to the TLD case is more complicated. Precisely because of the splitting that occurs in mode 1, a setting of order 3 (m=3 in eq. 1) is necessary. Figure 10a shows the stability diagram together with the fitted FRFs (10b) for this case. The values for the split mode 1 are also shown in the corresponding tables.

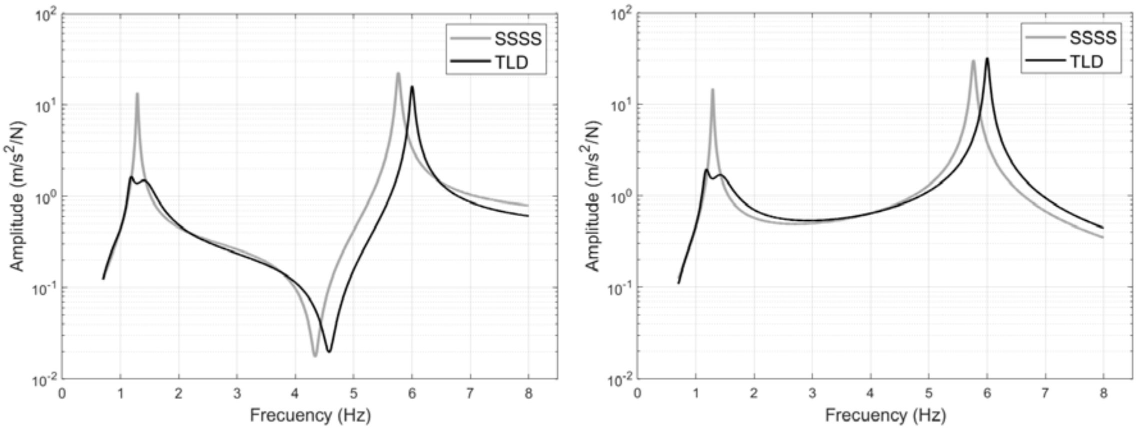

Figure 10b. Case TLD: FRF of the first floor (left) and of the second floor (right)

In order to better observe how the modal parameters evolve through the different cases, Figure 11 shows the accelerances of the first peak (in floor 1 and floor 2) together with the corresponding value of the frequency of the first mode (figure 11 a) and also the modal damping ratio (figure 11b). Similarly, figures 11c and 11d refer to the second mode.

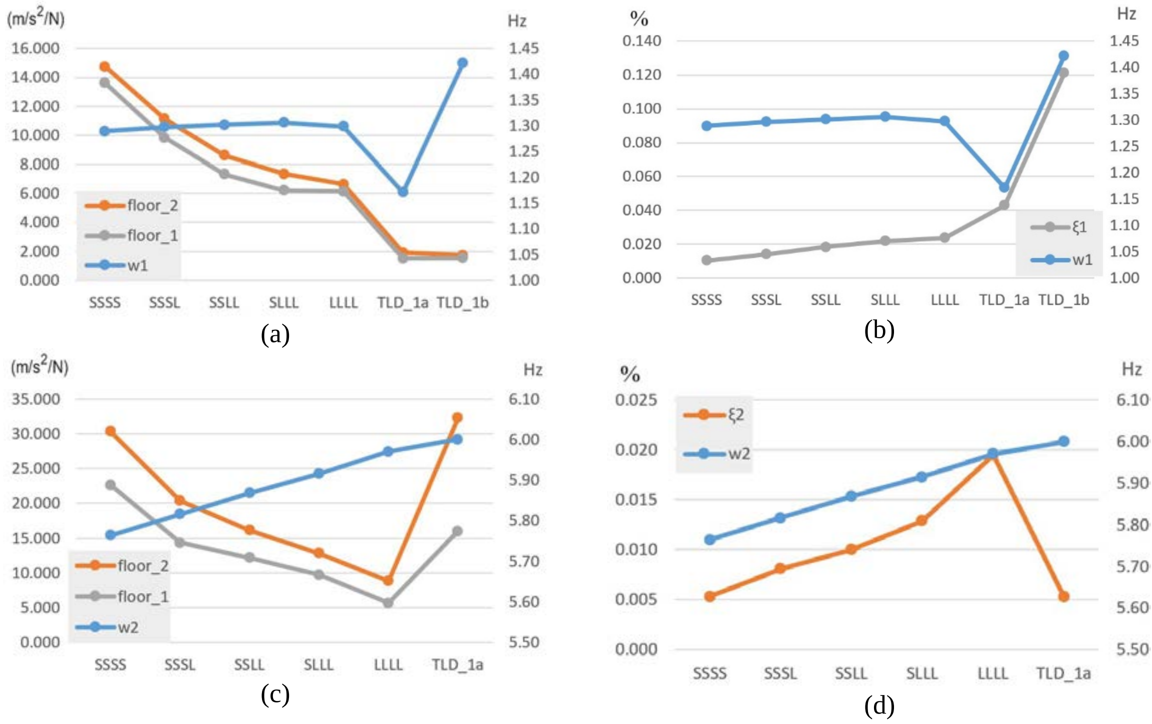

Figure 11. Trends for frequencies, accelerances and dampings

Once known the scaled modal coordinates (table 3) it is also possible to estimate the modal masses of each mode, which is shown in table 4 and plotted in figure 12.

	modal mass 1	modal mass 2
SSSS	3.007	2.323
SSSL	2.828	2.132
SSLL	2.690	2.323
SLLL	2.620	2.281
LLLL	2.936	1.819
TLD	2.867	1.479

Table 4. Modal masses for each case

Figure 12. Trends for modal masses.

5 CONCLUSIONS

As the load changes from solid to liquid, the frequency of the mode 1 remains sensibly constant (except in the split, TMD case) while the frequency of the mode 2 slightly increases (4%). Similarly, the accelerances decrease (55% on average, not counting on the TLD case) and the damping increases (up to 130% for mode 1 and 270% for mode 2, not counting on the TLD case). Modal masses do not have a defined trend.

All these interesting results must be carefully analysed. Similar experiments are proposed for vertical vibrations on the bridge scale model (figure 3). Full scale tests are also pending.

After the analysis of the estimated FRFs for all the scenarios, it will be concluded that the nature (solid or liquid) of the added mass affect the modal properties. It is known that the liquid mass can provide new natural modes. In the case the new modes are close to the ones of the original model, relevant changes could appear because of the interaction effects, being these phenomena similar to the working principle of the tuned liquid damper (case TLD, included).

Note that more cumbersome scenarios can appear when crowds occupy the floor structure [6, 7]. From the experiments carried out, it should be concluded that the typical static load test scenarios present some limitations when used to perform modal identifications or dynamic tests, since they may not describe the actual conditions of the structure during its normal use (live loading).

Acknowledgements

The authors wish to acknowledge the Ministerio de Economia y Competitividad, Spanish Government, for the partial support through the RTI2018-098425 Research Project and the Ministerio de Educacion, Cultura y Deporte, Spanish Government, for the FPU16/01339 predoctoral grant.

REFERENCES

[1] D. J. Ewins, Modal testing : theory, practice, and application. Research Studies Press, 2000.

[2] N. M. M. Maia and J. M. M. Silva, Theoretical and Experimental Modal Analysis. Research Studies Press, 1997.

[3] N.J. Bertola and I.F.C. Smith, A methodology for measurement-system design combining information from static and dynamic excitations for bridge load testing. Journal of Sound and Vibration (2019), 463

[4] M. Setareh and S. Gan, Vibration Testing, Analysis, and Human-Structure Interaction Studies of a Slender Footbridge. Journal of Performance of Constructed Facilities (2018), 32(5)

[5] J. A. Fabunmi, Spectral basis theory for the identification of structural dynamic systems, AIAA J., vol. 26, no. 6, pp. 726–732, 1988.

[6] A. Srikantha Phani and J. Woodhouse, Viscous damping identification in linear vibration, J. Sound Vib., vol. 303, no. 3–5, pp. 475–500, Jun. 2007.

[7] K. S. Kim, Y. J. Kang, and J. Yoo, Structural parameters identification using improved normal frequency response function method, Mech. Syst. Signal Process., vol. 22, no. 8, pp. 1858–1868, Nov. 2008.